# Dark Matter constraints from Fermi LAT inner Galaxy measurements

**Carlos Muñoz**

Instituto de Física Teórica UAM-CSIC

Departamento de Física Teórica

MultiDark
Multimessenger Approach for Dark Matter Detection

**HAP Dark Matter 2013,** Univ. Munster, February 18-20

By comparing theoretical predictions
with the gamma-ray emission observed by the Fermi LAT
from the region around the Galactic Center,

is it possible to derive stringent constraints on parameters
of generic dark matter (DM) candidates?

# INDIRECT DETECTION

- Annihilation of WIMPs in the galactic center will produce gamma rays

and these can be measured in space-based detectors

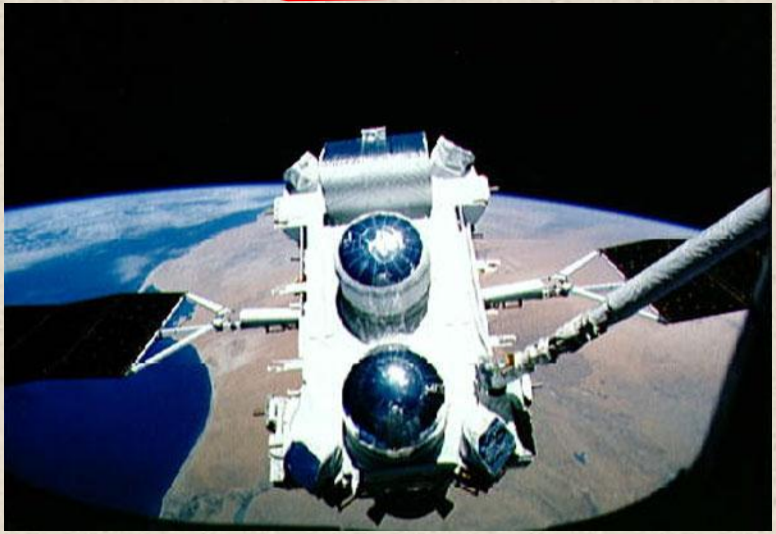

The Compton Gamma Ray Observatory (CGRO) satellite

EGRET telescope, after 5 years of mapping the gamma-ray sky, identified a gamma-ray source at the galactic center that, apparently, has no simple explanation with standard processes. In particular,

the flux is about $10^{-8}$ $cm^{-2}$ $s^{-1}$

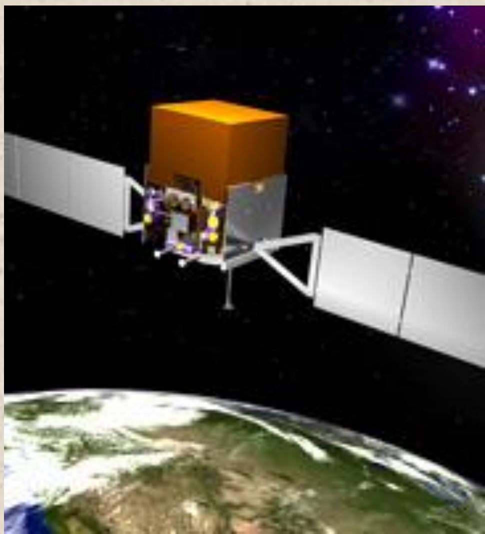

Starting in 2007, the GLAST satellite will be able to detect a flux of gamma rays, as small as $10^{-11}$ $cm^{-2}$ $s^{-1}$ , clarifying the situation

Old transparencies: Feb. 2006

As in the case of direct detection, it is also crucial for indirect detection to analyze the compatibility of the **neutralino** as a dark matter candidate, with the sensitivity of detectors

Old transparencies: Feb. 2006

# Theoretical Predictions

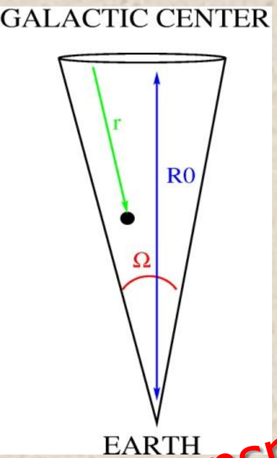


$\phi \sim (\int_{\text{line of sight}} \rho^2 \, dr) \; \sigma_{ann} v / m^2$

Astrophysics

Particle physics

Old transparencies: Feb. 2006

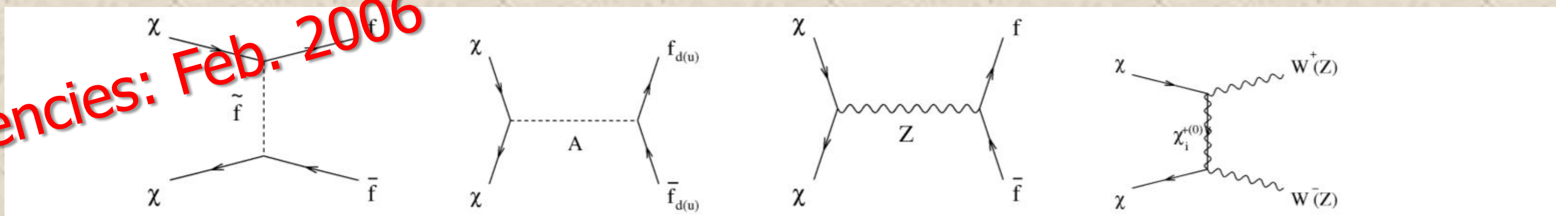


$\propto \frac{m_\chi m_f}{m_{\tilde f}^2} Z_{11}^2 \qquad \propto \frac{m_\chi^2}{m_A^2} \frac{Z_{11} Z_{13,14}}{m_W} m_{f_d} \tan\beta\left(\frac{m_{f_u}}{\tan\beta}\right) \qquad \propto \frac{m_f m_\chi}{m_Z^2} Z_{13,14}^2 \qquad \propto \frac{[-Z_{14}V_{21}^* + \sqrt{2} Z_{12} V_{11}^*]^2 (-Z_{13} N_{31}^* + Z_{14} N_{41}^*)^2}{1 + m^2_{\chi_i^{+(0)}}/m_\chi^2 - m^2_{W(Z)}/m_\chi^2}$

Particle physics:
Since the diagrams are related, we can use the same arguments as for direct detection

Astrophysics: e.g. a **NFW profile** for our galaxy, has for small distances from the galactic center $\rho(r) \sim \rho_0 / r$

E.g. for **$r = 0.01$ pc, $\rho(r) = \rho_0 \times 10^6$**

For **$m \sim 100$ GeV** and $\Omega_{DM} h^2 \sim 1/\sigma_{ann} \sim 0.1$ this implies the upper bound

$\phi \sim 10^{-9}\ \text{cm}^{-2}\ \text{s}^{-1}$ **i.e. below EGRET sensitivity**

However GLAST will be able to test some regions

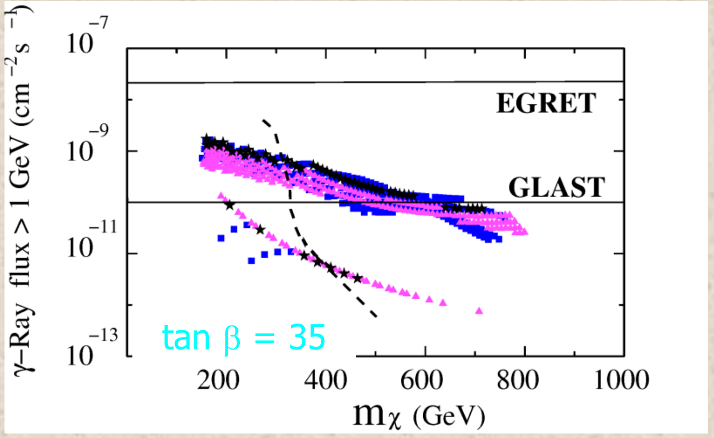


Old transparencies: Feb. 2006

# Baryons

- The previous situation occurs for simulations of halos without baryons. When baryons are taken into account a larger $\rho(r)$ is obtain, producing a larger $\phi$, and therefore increasing the dark matter detectability

Prada, Klypin, Flix Molina, Martinez, Simonneau, 0401512

a NFW profile including baryons has $\rho(r) \sim \rho_0/r^{1.45}$, producing $\phi$ **x 100**

Mambrini, Munoz, Nezri, Prada, 0506204

Old transparencies: Feb. 2006

# GLAST

Even for CMSSM, points corresponding to tan β=5 will be reached by GLAST

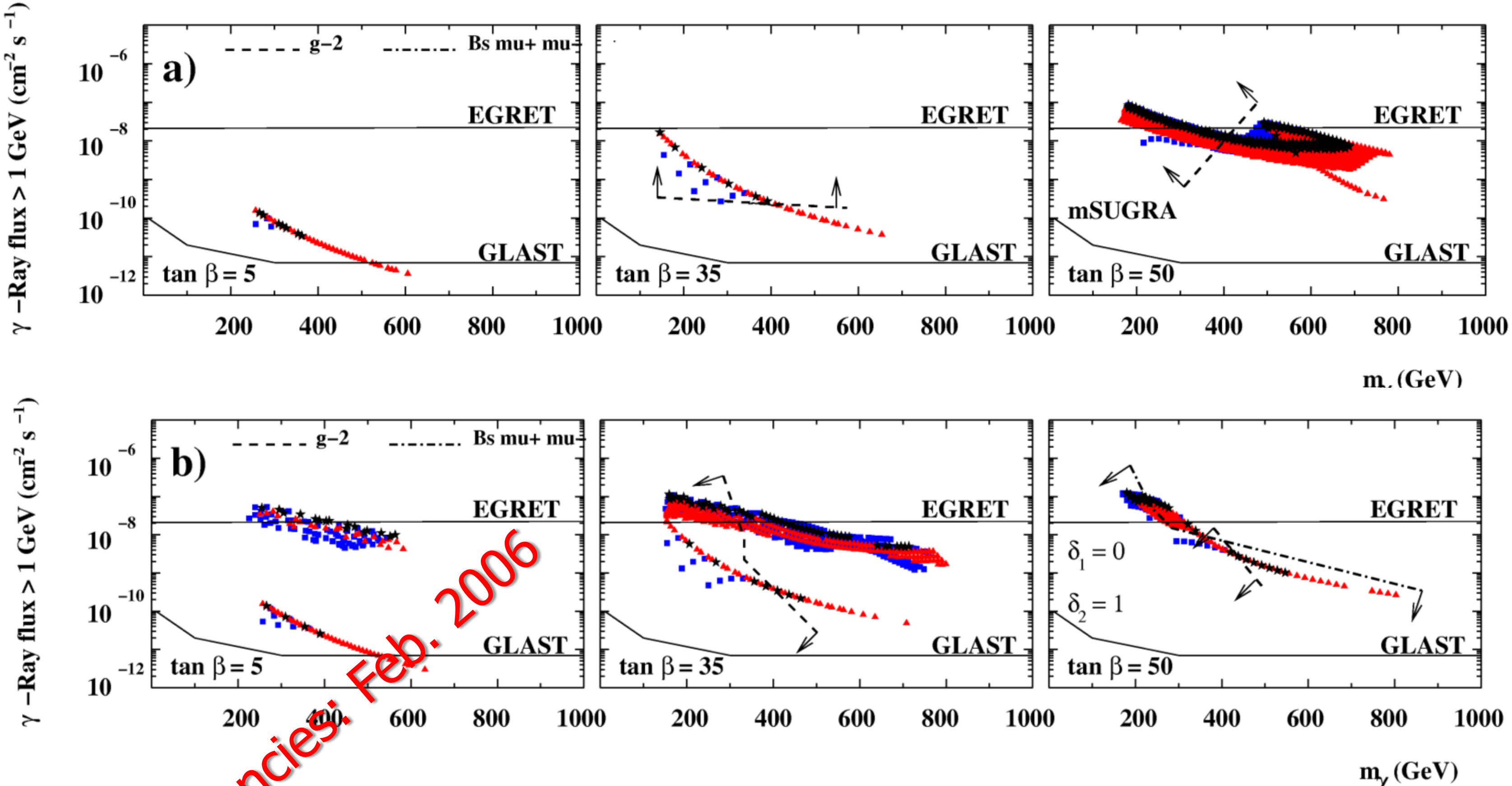


Thus, important regions of the parameter space of MSSM will be tested by GLAST

Mambrini, Munoz, Nezri, Prada, 0506204

By comparing theoretical predictions
with the gamma-ray emission observed by the Fermi LAT
from the region around the Galactic Center,

is it possible to derive stringent constraints on parameters of
generic dark matter (DM) candidates?

YES in the likely case that the collapse of baryons to the Galactic Center
is accompanied by the contraction of the DM:

Cerdeño, Huh, Klypin, Mambrini, C.M., Peiró, Prada, Gómez-Vargas, Morselli, Sánchez-Conde — MultiDark + Fermi

**Preliminary results: December 2012**

The analysis is conservative since it simply requires that the expected DM signal does not exceed the observed gamma-ray emission (due to DM + astrophysical background)

The upper limits on the annihilation cross section of DM particles obtained are two orders of magnitude stronger than withouth contraction

# DARK MATTER DENSITY PROFILES

High-resolution N-body simulations of the gravitational collapse of a collisionless system of particles, suggest the existence of a universal DM density profile.

from micro-haloes to galaxy clusters

Using the parametrization:

$$\rho(r) = \frac{\rho_s}{\left(\frac{r}{r_s}\right)^{\gamma}\left[1+\left(\frac{r}{r_s}\right)^{\alpha}\right]^{\frac{\beta-\gamma}{\alpha}}},$$

where the density $\rho_s$ and the radius $r_s$ vary from halo to halo

- The NFW profile, with $(\alpha,\beta,\gamma)=(1,3,1)$, is the most widely used

Navarro, Frenk, White, 9508025, 9611107

$$\rho(r) = \frac{\rho_s}{(r/r_s)\,(1 + r/r_s)^2}$$

Cuspy profile in the inner region ( $\rho_h \longrightarrow 1/r$ ) implying a singularity towards the center

- Another approximation is the so-called Einasto profile which seems to provide a better fit than NFW to numerical results

Einasto, 1968
Navarro et al., 0311231

$$\rho_{\rm Ein}(r) = \rho_s \exp\left\{-\frac{2}{\alpha}\left[\left(\frac{r}{r_s}\right)^{\alpha} - 1\right]\right\},$$

Simulations now resolve the cusp down to radius of ~ 100 pc, thus there is less of extrapolation to the central region of ~ 1-10 pc, where most of the annihilation signal is expected to come from

But these are DM-only simulations, and central regions of galaxies like the Milky Way are dominated by baryons

They might modify e.g. the behaviour of NFW $\rho \longrightarrow 1/r$ making it steeper

The baryons lose energy through radiative processes and fall into the central regions of a forming galaxy. Thus the resulting gravitational potential is deeper, and the DM must move closer to the center increasing its density

Zeldovich, Klypin, Khlopov, Chechetkin, 1980
Blumenthal, Faber, Flores, Primack, 1986
Gnedin, Kravtsov, Klypin, Nagai, 0406247

The effect seems to be confirmed by high-resolution hydrodynamic simulations that self-consistently include complex baryonic physics such as gas dissipation, star formation and supernova feedback

Gustafsson, Fairbairn, Sommmer-Larsen, 0608634
Colín, Valenzuela, Klypin, 0506627
Tissera, White, Pedrosa, Scannapieco, 0911.2316
O.Y. Gnedin, Ceverino, N.Y. Gnedin, Klypin, Kravtsov, Levine, Nagai, Yepes, 1108.5736

From observational data of the Milky Way, the parameters of the DM profiles have been constrained

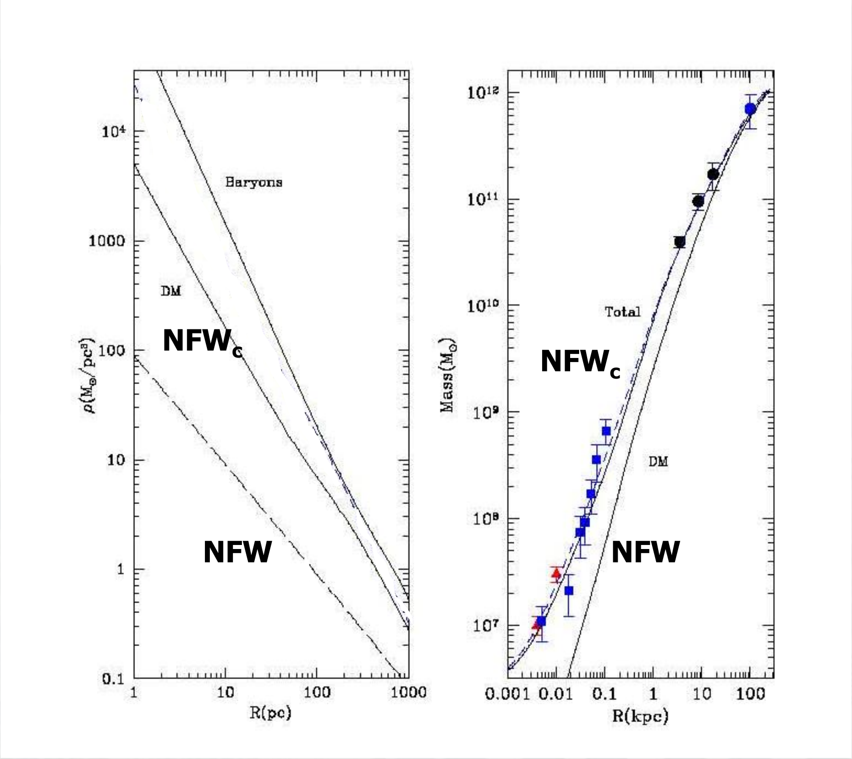


Prada, Klypin, Flix Molina, Martínez, Simonneau, astro-ph/0401512

Fitting the data with the power-law parametrization:

Cerdeño, Huh, Klypin, Mambrini, C.M., Peiró, Prada, Gómez-Vargas, Morselli, Sánchez-Conde

MultiDark + Fermi

**Preliminary results: December 2012**

$$\rho_{NFW}(r) = \frac{\rho_s}{(r/r_s)\,(1 + r/r_s)^2} \rightarrow \rho_{NFWc}(r) = \frac{\rho_s}{(r/r_s)^{1.37}\,[1 + (r/r_s)^{0.76}]^{2.54}}$$

- in the inner region $\rho \rightarrow 1/r$ → in the inner region $\rho \rightarrow 1/r^{1.37}$

| Profile | $\alpha$ | $\beta$ | $\gamma$ | $\rho_s$ [GeV cm$^{-3}$] | $r_s$ [kpc] |
|---|---|---|---|---|---|
| NFW | 1 | 3 | 1 | 0.21 | 23.8 |
| NFW$_c$ | 0.76 | 3.3 | 1.37 | 0.35 | 18.5 |
| Einasto | 0.22 | — | — | 0.08 | 19.7 |

Catena, Ullio, 0907.0018 →

## Caution:

Astrophysicists identified another process, which tends to decrease the DM density and flatten the DM cusp

Mashchenko, Couchman, Wadsley, 0605672, 0711.4803
Pontzen, Governato, Blumenthal, 1106.0499

The mechanism relies on numerous episodes of baryon infall followed by a strong burst of star formation, which expels the baryons producing at the end a significant decline of the DM density.

Cosmological simulations which implement this process show this result

Governato et al., 0911.2237
Maccio et al, 1111.5620

Whether the process happened in reality in the Milky Way is still unclear…

# GAMMA-RAY FLUX FROM DARK MATTER ANNIHILATION

$$\left(\frac{d\Phi_\gamma}{dE_\gamma}\right)_{prompt} = \sum_i \frac{dN_\gamma^i}{dE_\gamma} \frac{\langle\sigma_i v\rangle}{8\pi m_{DM}^2} \bar{J}(\Delta\Omega)\Delta\Omega \,,$$

$$\bar{J}(\Delta\Omega) \equiv \frac{1}{\Delta\Omega}\int d\Omega \int_{l.o.s.} \rho^2(r(l,\Psi))\, dl \,.$$

The theory

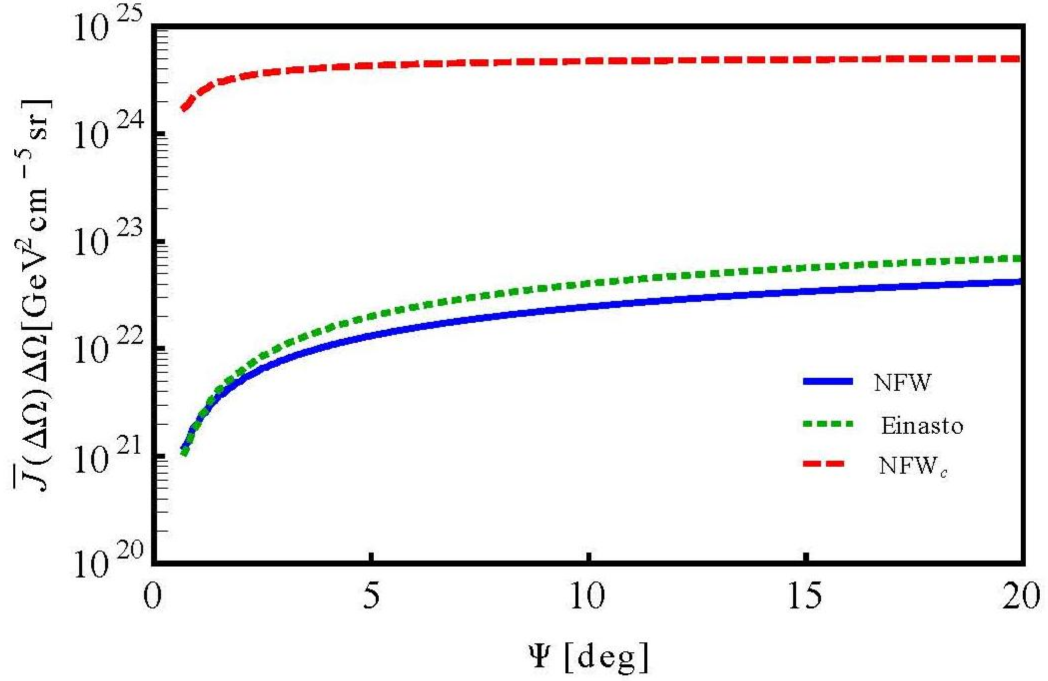


Figure 1: The $\bar{J}(\Delta\Omega)\Delta\Omega$ quantity integrated on a ring with inner radius of 0.5 degrees and external radius of $\Psi$ degrees for the DM density profiles given in Table 1. Blue (solid), red (long-dashed) and green (short-dashed) lines correspond to NFW, $\mathrm{NFW}_c$ and Einasto profiles, respectively. The three density profiles are compatible with current observational data.

# GAMMA-RAY FLUX FROM Fermi LAT MEASUREMENTS

Credit: NASA/General Dynamics

The experiment

Launched in June 2008

The LAT covers an energy range from ~20 MeV to > 300 GeV
with a large effective area (~6500 cm$^2$) above 1 GeV
and a large field of view (2.4 sr)

# Optimization of the region of interest for dark matter searches

In order to find the ROI that maximizes the S/N, we follow the next steps:

1. Maps of the quantity $\bar{J}(\Delta\Omega)\,\Delta\Omega$ for the three DM density profiles considered (i.e., Einasto,NFW and NFWc) are built, and used as the signal.
2. The noise is assumed to be the square root of the photon flux map, as measured by Fermi.
3. A mask is introduced to cover the GC and the Galactic plane, i.e., the most conflictive regions in the analysis.

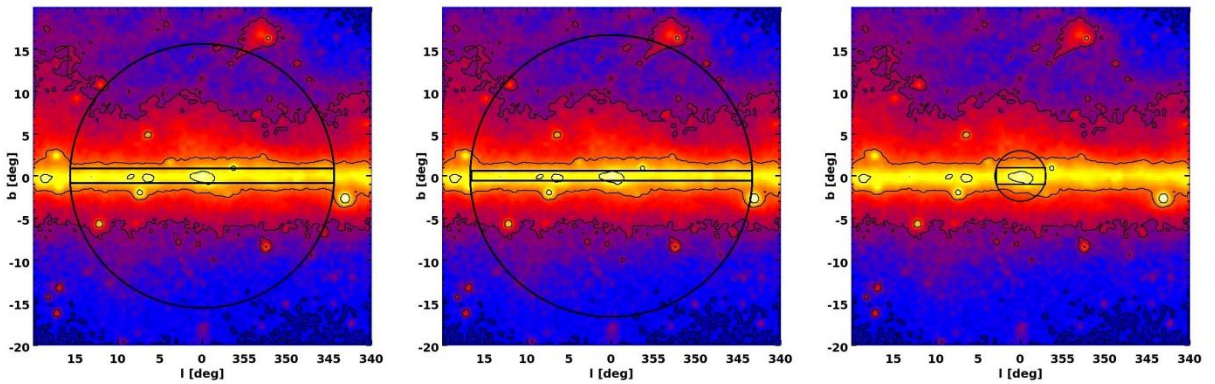


Figure 3: Maps of the observed flux by the Fermi-LAT in the energy range 1 − 100 GeV, in units of photons cm$^{-2}$ s$^{-1}$, for the three DM profiles studied. From left to right: Einasto, NFW and NFW$_c$.

| Profile | $\theta_2$ [deg] | $\|b\|$ [deg] | $\Delta\Omega$ [sr] | $\bar{J}(\Delta\Omega)\,\Delta\Omega$ [$\times 10^{22}$ GeV$^2$ cm$^{-5}$ sr] | Flux (1 − 100 GeV) [$\times 10^{-7}$ cm$^{-2}$s$^{-1}$] |
|---|---|---|---|---|---|
| Einasto | 15.6 | 0.7 | 0.217 | 5.1 | $31.4 \pm 0.3$ |
| NFW | 16.7 | 0.6 | 0.253 | 3.3 | $38.0 \pm 0.3$ |
| NFW$_c$ | 3.0 | 1.0 | 0.005 | 86.8 | $2.2 \pm 0.1$ |


Carlos Muñoz
UAM & IFT

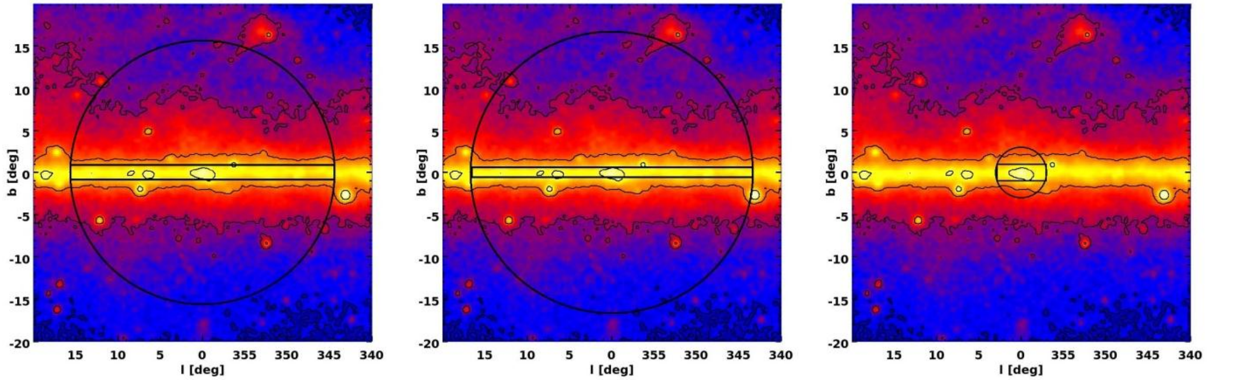


Figure 3: Maps of the observed flux by the Fermi-LAT in the energy range $1 - 100$ GeV, in units of photons $cm^{-2}$ $s^{-1}$, for the three DM profiles studied. From left to right: Einasto, NFW and $NFW_c$.

Clearly, the $NFW_c$ ROI is the smallest one. This is because in the inner region of 5 deg, the $J(\Delta\Omega)\ \Delta\Omega$ for $NFW_c$ becomes constant, whereas for the other two profiles this quantity becomes flat at larger radius. Therefore, by increasing the aperture above few degrees does not increase the S/N for the NFWc case

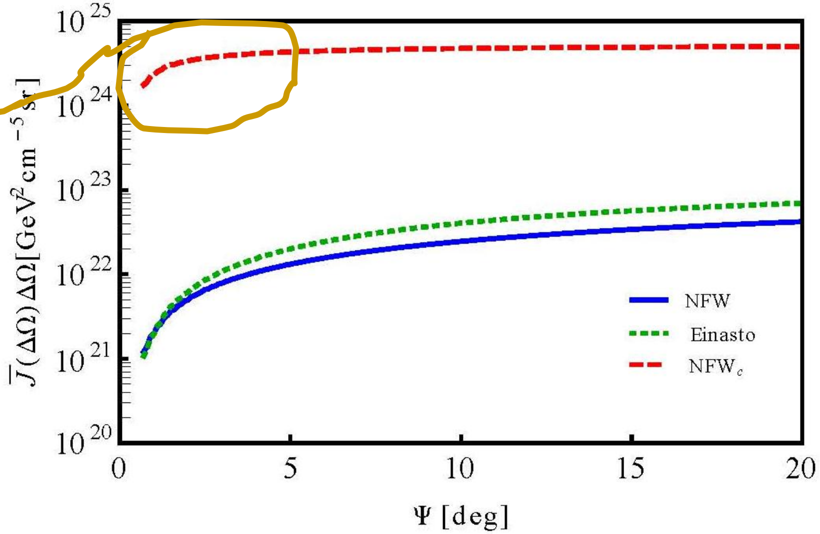


Figure 1: The $\bar{J}(\Delta\Omega)\Delta\Omega$ quantity integrated on a ring with inner radius of 0.5 degrees and external radius of $\Psi$ degrees for the DM density profiles given in Table 1. Blue (solid), red (long-dashed) and green (short-dashed) lines correspond to NFW, $NFW_c$ and Einasto profiles, respectively. The three density profiles are compatible with current observational data.

# Flux measurement

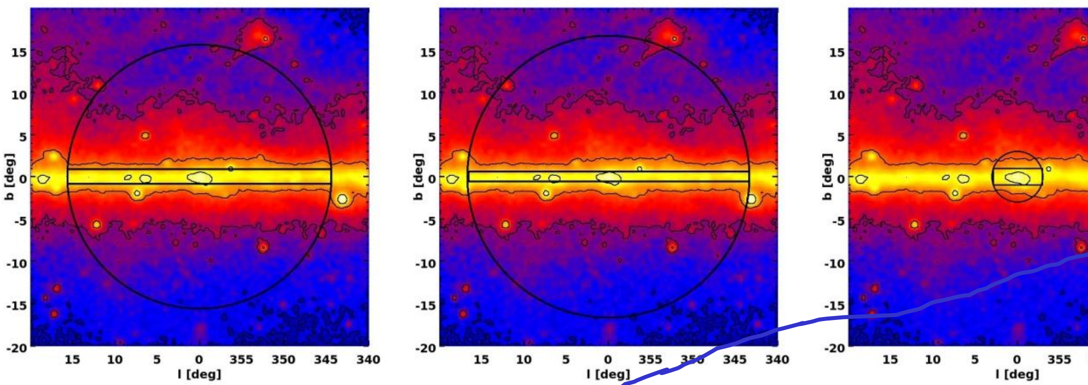


Figure 3: Maps of the observed flux by the Fermi-LAT in the energy range 1 – 100 GeV, in units of photons $cm^{-2}$ $s^{-1}$, for the three DM profiles studied. From left to right: Einasto, NFW and $NFW_c$. I

| Profile | $\bar{J}(\Delta\Omega)\,\Delta\Omega$ $[\times 10^{22}$ GeV$^2$ cm$^{-5}$ sr$]$ | Flux (1 – 100 GeV) $[\times 10^{-7}$ cm$^{-2}$s$^{-1}]$ |
|---|---|---|
| Einasto | 5.1 | $31.4 \pm 0.3$ |
| NFW | 3.3 | $38.0 \pm 0.3$ |
| $NFW_c$ | 86.8 | $2.2 \pm 0.1$ |

To set constraints we request that the DM-induced gamma ray flux does not exceed the observed flux upper limit

No subtraction of any astrophysical background is made

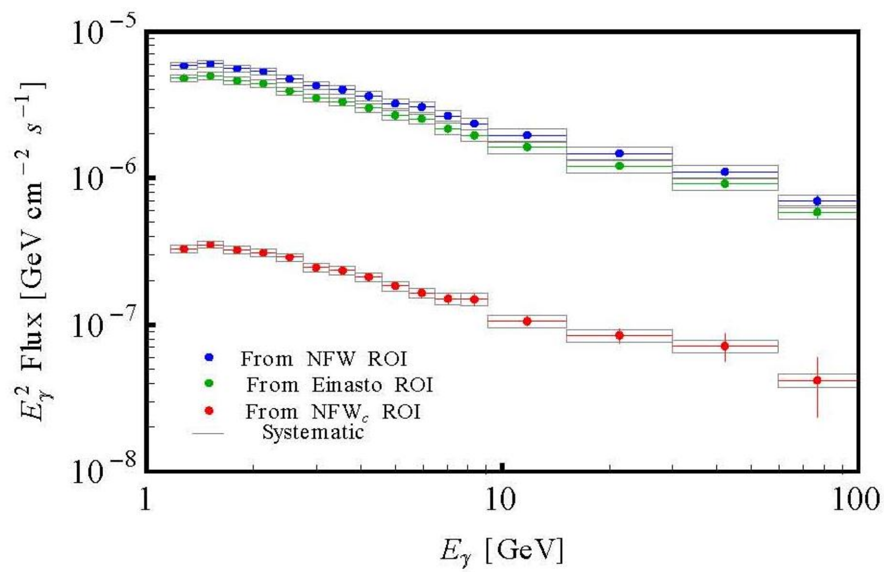


Figure 4: Energy spectrum extracted from Fermi-LAT data for the optimized regions that are shown in Figure 3. Data are shown as points and the vertical error bars represent the statistical errors. The latter are in many cases smaller than the point size. The boxes represent the systematic error in the Fermi-LAT effective area.


Carlos Muñoz
UAM & IFT

# LIMITS ON THE DARK MATTER ANNIHILATION CROSS SECTION

Conservative approach:
Require that the integrated gamma-ray flux of the expected DM signal for each energy bin does not exceed the observed flux upper limit

No subtraction of any astrophysical background is made

We use LAT data measured between August 4, 2008, and June 15, 2012

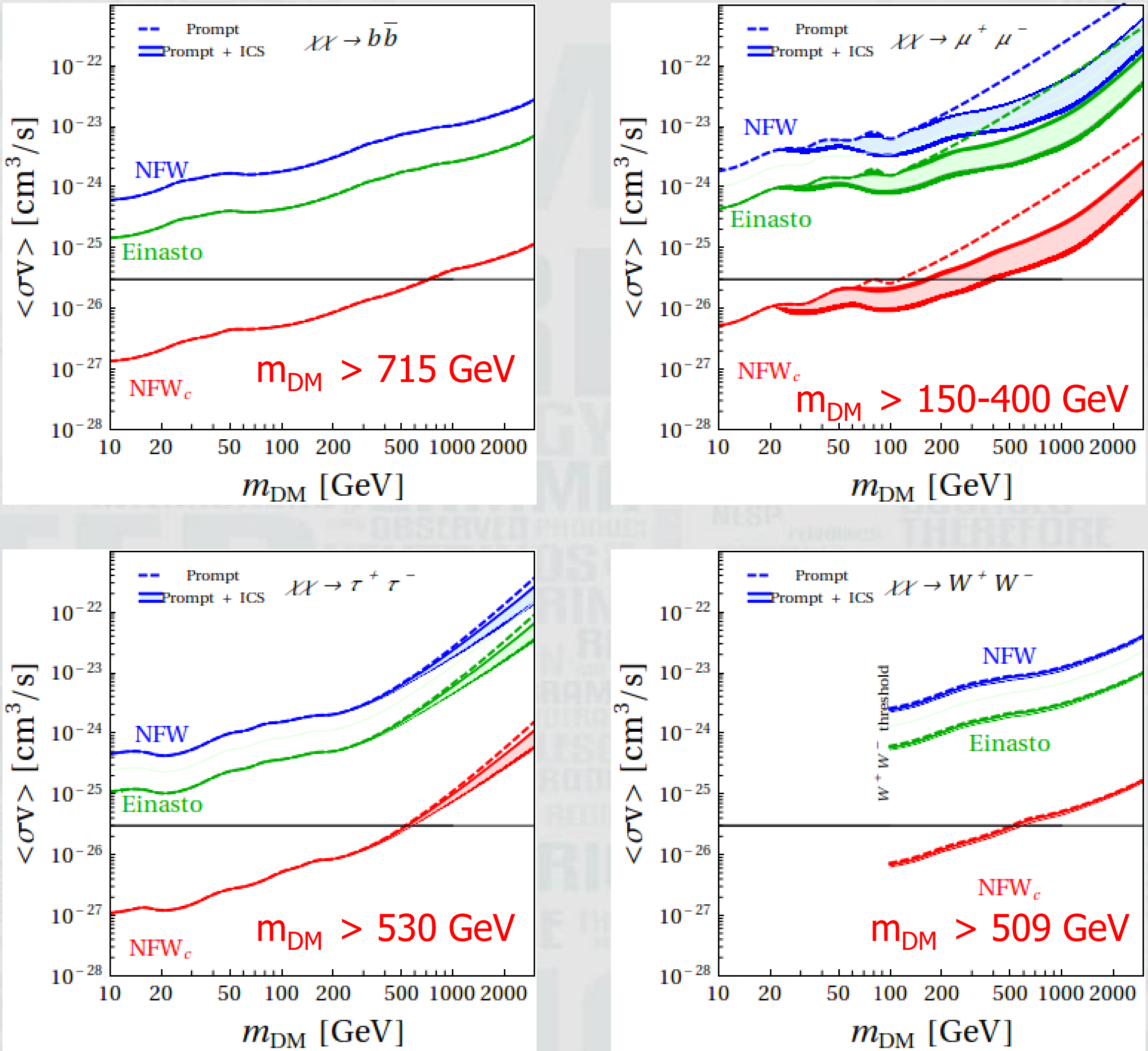


Figure 5: $3\sigma$ upper limits on the annihilation cross-section of models in which DM annihilates into $b\bar{b}$, $\mu^+\mu^-$ (upper pannel), $\tau^+\tau^-$ and $W^+W^-$ (lower pannel), for the three DM density profiles discussed in the text. Upper limits set without including the ICS component in the computation are also given as dashed curves (prompt) for comparison. The uncertainty in the diffusion model is shown as the thickness of the solid curves (from top to bottom: MIN, MED, MAX) while the lighter shaded regions represent the impact of the different strength of the Galactic magnetic field with lower(higher) values of the cross-section corresponding to $B_0 = 1\ \mu$G($B_0 = 10\ \mu$G). The horizontal line corresponds to the expected value of the thermal cross-section for a generic WIMP candidate.

In general the final state will be a combination of the final states presented here.

e.g., in SUSY, the neutralino annihilation modes are 70% bb - 30% ττ for a Bino DM, and 100% $W^+W^-$ for a Wino DM (or for a Higgs-portal model)

Also, the value of σv in the Galactic halo might be smaller than $3 \times 10^{-26}$ cm$^3$ s$^{-1}$

e.g., in SUSY, in the early Universe coannihilation channels can also contribute to σv.

Also, DM particles whose annihilation in the Early Universe is dominated by velocity dependent contributions would have a smaller value of σv in the Galactic halo, where the DM velocity is much smaller, and can escape this constraint.

$\Omega h^2 \approx 3 \times 10^{-27}\ \mathrm{cm}^3\ \mathrm{s}^{-1}\ \langle\sigma v\rangle^{-1} \approx 0.1.$

In this sense, the results derived for pure annihilation channels can be interpreted as limiting cases which give an idea of what can happen in realistic scenarios

Work in progress:
Analysis of the SUSY parameter space by:

Cerdeño, Huh, Klypin, Mambrini, C.M., Peiró, Prada,
Gómez-Vargas, Morselli, Sánchez-Conde

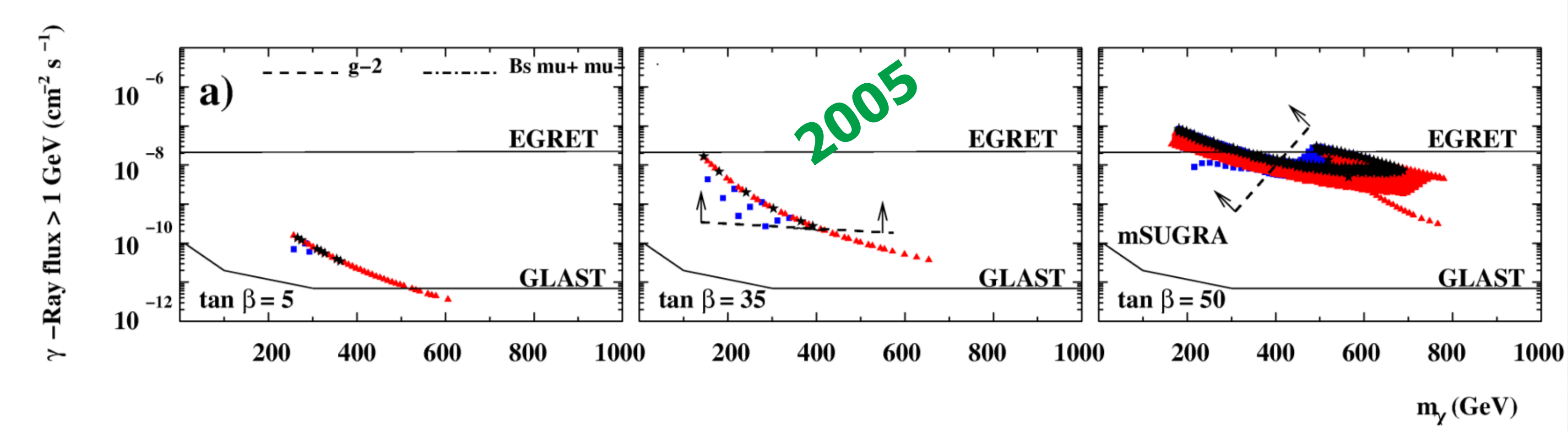

# CONCLUSIONS

Fermi LAT data imply that large regions of parameters of DM candidates are not compatible with compressed DM density profiles

e.g.:

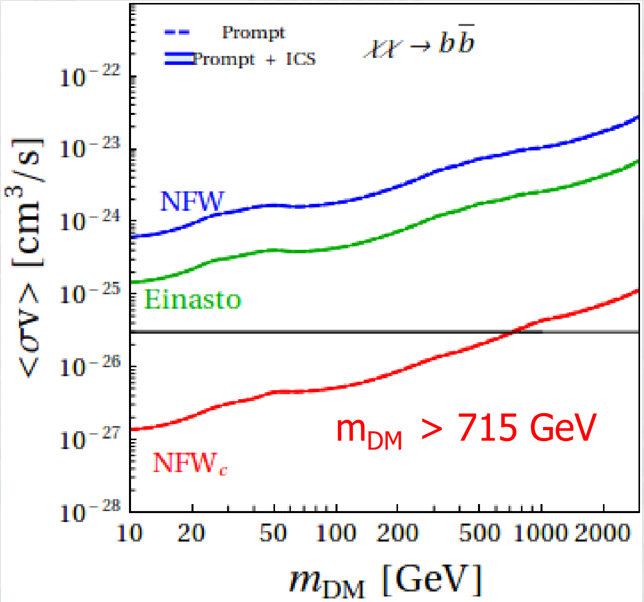


THE END

Carlos Muño

# BACKUP SLIDES

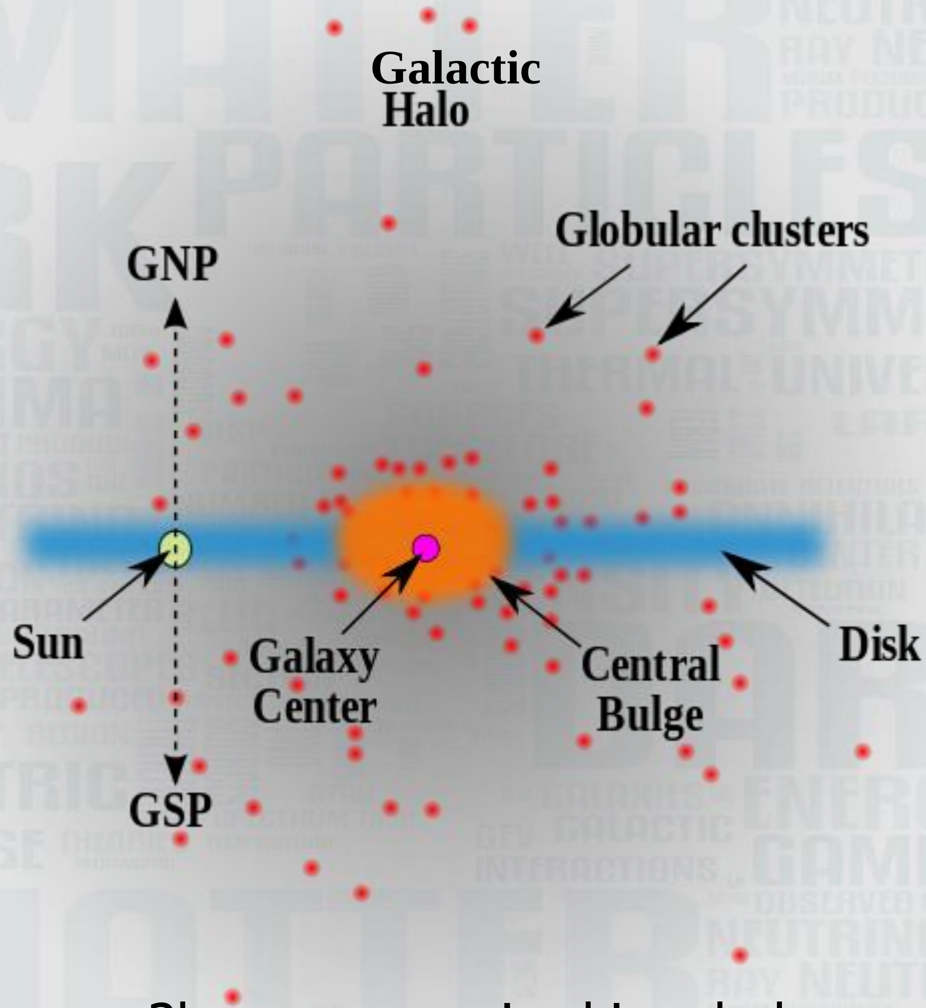


The stars in the inner ≈ 3kpc are organized in a bulge and the bar

In the Galactic Center there is a supermassive black hole ≈ 2.6 x $10^6$ $M_\odot$

| TABLE I: | constraints for the Milky Way Galaxy |
|---|---|
| | Constr. |
| Virial mass, $10^{12} M_\odot$ | – |
| Virial radius, kpc | – |
| Halo concentration C | 10.3-21.5 (1.5$\sigma$) |
| Disk mass, $10^{10} M_\odot$ | – |
| Disk scale length, kpc | 2.5-3.5 |
| Bulge mass, $10^{9} M_\odot$ | – |
| Black Hole mass, $10^{6} M_\odot$ | 2.6 |
| $M(< 100\text{kpc})$, $10^{11} M_\odot$ | $7.5 \pm 2.5$ |
| $\Sigma_{\text{total}}$, $\lvert z \rvert < 1.1$ kpc at $R_\odot$, $M_\odot \text{pc}^{-2}$ | $71 \pm 6$ |
| $\Sigma_{\text{baryon}}$ at $R_\odot$,$M_\odot \text{pc}^{-2}$ | $48 \pm 8$ |
| $V_{\text{circ}}$ at 3 kpc, km/s | $200 \pm 5$ |

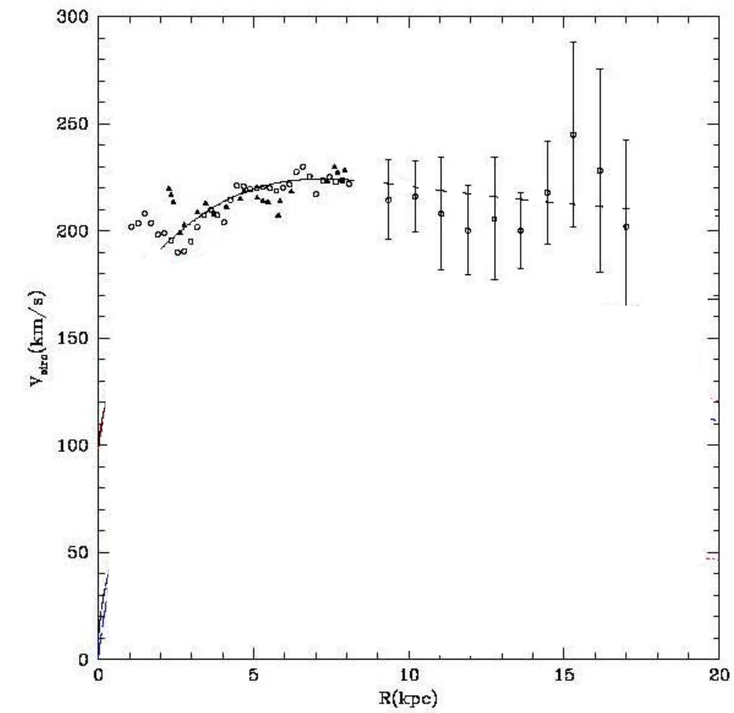


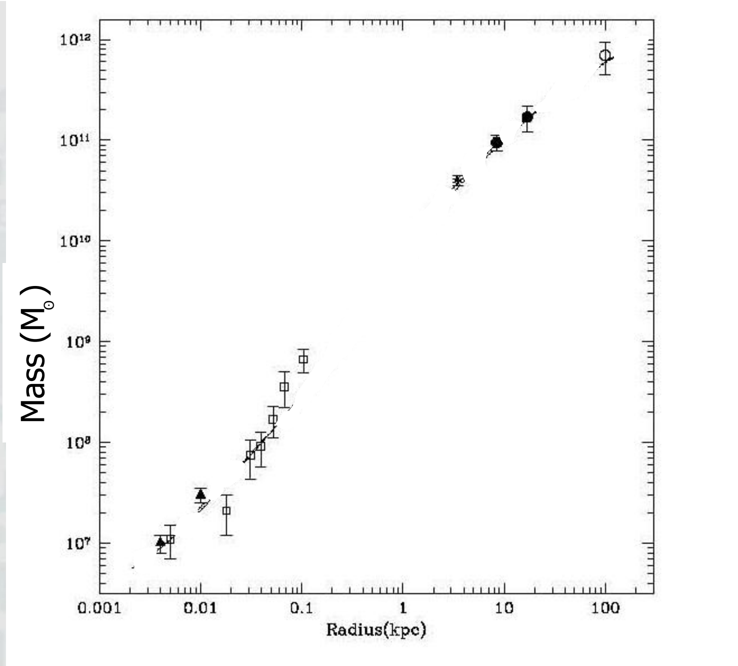


Klypin, Zhao, Somerville, astro-ph/0110390

TABLE I: Model and constraints for the Milky Way Galaxy

| | NFW | Constr. |
|---|---|---|
| Virial mass, $10^{12} M_\odot$ | 1.07 | – |
| Virial radius, kpc | 264 | – |
| Halo concentration C | 11 | 10.3-21.5 $(1.5\sigma)$ |
| Disk mass, $10^{10} M_\odot$ | 3.7 | – |
| Disk scale length, kpc | 3.2 | 2.5-3.5 |
| Bulge mass, $10^{9} M_\odot$ | 8.0 | – |
| Black Hole mass, $10^{6} M_\odot$ | 2.6 | 2.6 |
| $M(< 100\text{kpc})$, $10^{11} M_\odot$ | 6.25 | $7.5 \pm 2.5$ |
| $\Sigma_{\text{total}}$, $\lvert z\rvert < 1.1$ kpc at $R_\odot$, $M_\odot \text{pc}^{-2}$ | 65 | $71 \pm 6$ |
| $\Sigma_{\text{baryon}}$ at $R_\odot$, $M_\odot \text{pc}^{-2}$ | 47 | $48 \pm 8$ |
| $V_{\text{circ}}$ at 3 kpc, km/s | 203 | $200 \pm 5$ |

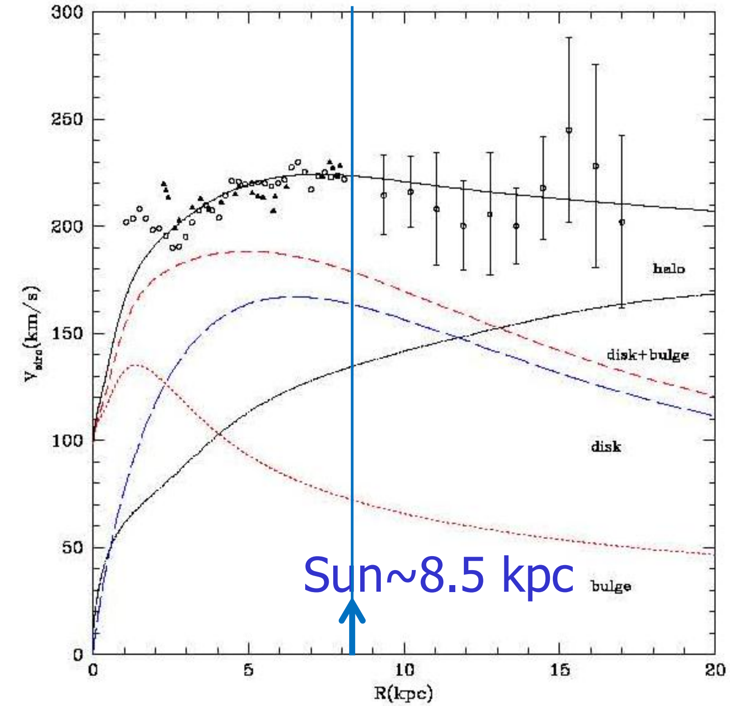


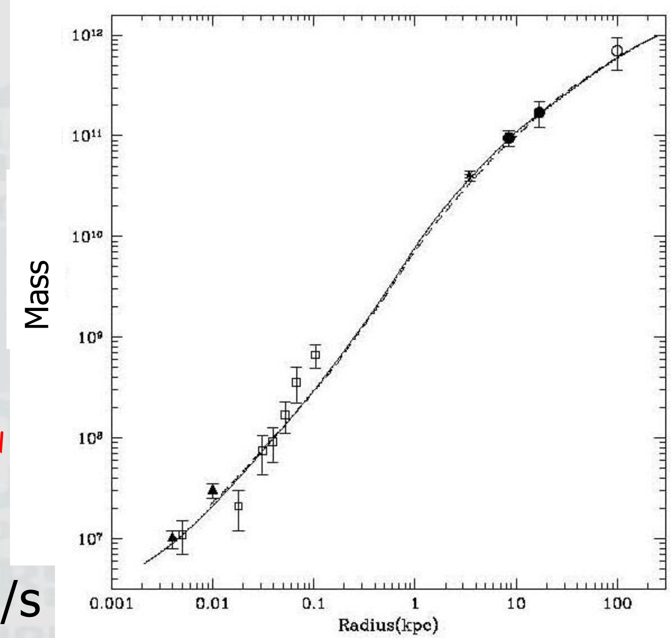


$$\rho_h(r) = \frac{\rho_s}{(r/r_s)(1 + r/r_s)^2}$$

$\rho_s = 0.15\ \text{GeV/cm}^3$ $r_s = 23.8$ kpc

$r = 8.5$ kpc $\longrightarrow \rho_h(8.5) \equiv \rho_o = 0.23\ \text{GeV/cm}^3$

$V_0\,(8.5)_{\text{baryons}} \sim 180$ km/s ; $V_0\,(8.5)_{\text{total}} \sim 220$ km/s

## The effect of baryons in the distribution of dark matter

$$\rho_h(r) = \frac{\rho_s}{(r/r_s)\,(1 + r/r_s)^2}$$

This result is obtained from dark-matter-only simulations

When normal gas ("baryons") loses its energy through radiative processes, it falls to the central region of forming galaxy. As the result of this redistribution of mass, the gravitational potential **in the center** changes substantially. The dark matter must react to this deeper potential by moving closer to the center and **increasing its density**.

Assuming that the compression occurs adiabatically, one obtains:

$$M_i\,(r_i)\,r_i = M_f\,(r_f)\,r_f \quad , \quad M_f = M_{DM} + M_b$$

Mass profile of the galactic halo before the compression (obtained through N-body simulations)

$$M_i = M_{DM}\,(\Omega_{DM} + \Omega_b)\,/\,\Omega_{DM}$$

Baryonic composition of the Milky Way observed now

The to be determined dark matter component of the halo today

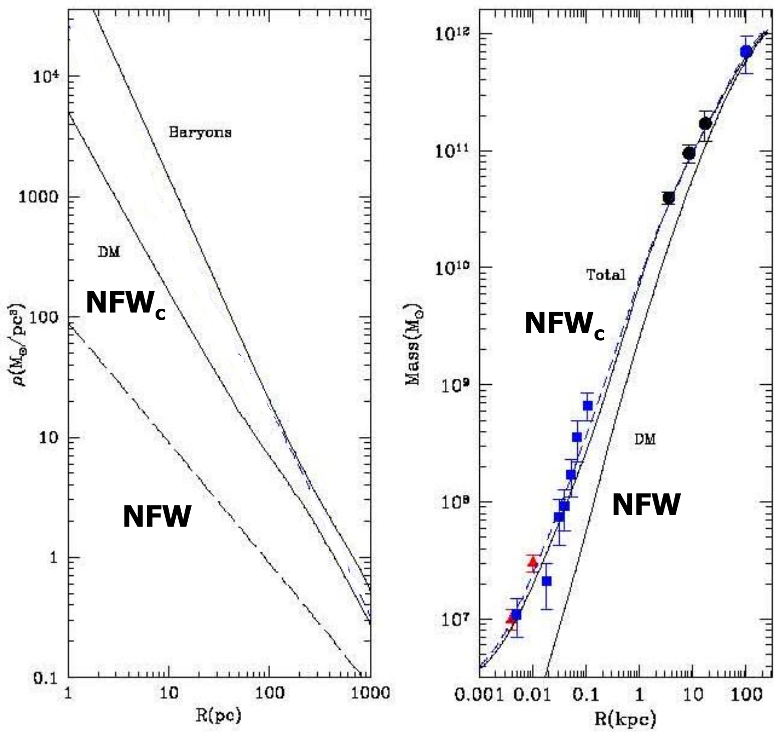


Prada, Klypin, Flix, Martínez, Simonneau, astro-ph/0401512

**NFW** → **NFW$_c$**

$$\rho_h(r) = \frac{\rho_s}{(r/r_s)\,(1 + r/r_s)^2} \longrightarrow \rho_h(r) = \frac{\rho_s}{(r/r_s)^{1.37}\,[1 + (r/r_s)^{0.76}]^{2.54}}$$

$\rho_s = 0.15$ GeV/cm$^3$ $r_s = 23.8$ kpc ⟶ $\rho_s = 0.35$ GeV/cm$^3$ $r_s = 18.5$ kpc

$r = 8.5$ kpc ⟶ $\rho_o = 0.23$ Gev/cm$^3$ ⟶ $r = 8.5$ kpc ⟶ $\rho_o = 0.33$ Gev/cm$^3$

- in the inner region $\rho_h \rightarrow 1/r$ ⟶ in the inner region $\rho_h \rightarrow 1/r^{1.37}$

Mambrini, C.M., Nezri, Prada, hep-ph/0506204

Gomez-Vargas et al., in preparation